Evolution of attractors in quasiperiodically forced systems: From quasiperiodic to strange nonchaotic to chaotic

Mingzhou Ding, Celso Grebogi, and Edward Ott
Laboratory for Plasma Research, University of Maryland, College Park, Maryland 20742
(Received 15 September 1988)

As a model displaying typical features of two-frequency quasiperiodically forced systems, we discuss the circle map with quasiperiodic coupling. We present numerical and analytical evidence for the existence of strange nonchaotic attractors, and we use examples to illustrate various types of dynamical behavior that can arise in typical quasiperiodically forced systems. We investigate the behavior of the system in the two-dimensional parameter plane of nonlinearity strength versus one of the driving frequencies. We find that the set in this parameter plane for which the system exhibits strange nonchaotic attractors has Cantor-like structure and is enclosed between two critical curves. One of these curves marks the transition from three-frequency quasiperiodic attractors to strange nonchaotic attractors; the other marks the transition from strange nonchaotic attractors to chaotic attractors. This suggests a possible route to chaos in two-frequency quasiperiodically forced systems: (three-frequency quasiperiodicity)→(strange nonchaotic behavior)→(chaos).

I. INTRODUCTION

Maps of a circle to itself are highly relevant models for understanding many interesting physical phenomena. The most frequently studied of such maps is

$$\phi_{n+1}=[\phi_n+2\pi K+V\sin\phi_n]\ , \tag{1}$$

where K and V are real parameters, and we henceforth use the square brackets to indicate that modulo 2π of the enclosed expression is taken. As K and V vary Eq. (1) exhibits a wealth of nonlinear dynamical phenomena: chaotic attractors, mode locking, period-doubling cascades, quasiperiodicity, intermittency, crisis, etc.[1] Past work shows that simple models, such as Eq. (1), exhibit features that are typical of more complex and realistic systems.

Our primary concern in this study is to understand how nonlinear systems respond to quasiperiodic forcing.[2–6] As a model to reveal typical features to be expected in this case, we consider a generalization of Eq. (1),

$$\phi_{n+1}=[\phi_n+2\pi K+V\sin\phi_n+C\cos\theta_n]\ , \tag{2}$$

$$\theta_{n+1}=[\theta_n+2\pi\omega]\ , \tag{3}$$

where K, V, and C are three parameters and ω is irrational. In our numerical experiments we used the reciprocal of the golden mean for ω, namely, $\omega=(\sqrt{5}-1)/2$. To motivate the form used in Eqs. (2) and (3) consider a continuous time system which is quasiperiodically driven at two incommensurate frequencies. Take the following pendulum equation as a typical example:

$$\frac{d^2\phi(t)}{dt^2}+\nu\frac{d\phi(t)}{dt}+g\sin\phi(t)=F+G\sin(\omega_1 t+\alpha_1)+H\sin(\omega_2 t+\alpha_2)\ , \tag{4}$$

where ω_1 and ω_2 are incommensurate. If we sample the system at time intervals corresponding to one of the driving frequencies, say, $\omega_1 t_n=2\pi n$, we obtain a discrete map for the variables $\phi,\theta=\omega_2 t$ and $\dot\phi=d\phi/dt$. The form of this discrete map is $\phi_{n+1}=\tilde F(\phi_n,\theta_n,\dot\phi_n)$, $\dot\phi_{n+1}=\tilde G(\phi_n,\theta_n,\dot\phi_n)$, $\theta_{n+1}=[\theta_n+2\pi\omega]$, where $\omega=\omega_2/\omega_1$. For not too small ν much of the dynamics of (4) can be modeled by neglecting the dependence of $\tilde F$ on $\dot\phi_n$, in which case the map has the same form as Eqs. (2) and (3).

It was shown in Ref. 3 that quasiperiodically forced systems can exhibit strange nonchaotic attractors. These attractors are not a finite set of points, or a smooth curve or surface, or a volume bounded by a piecewise smooth closed surface. Hence they are strange geometrically. On the other hand, a typical orbit on a strange nonchaotic attractor has nonpositive Lyapunov exponents. Therefore, they are nonchaotic in the sense that they do not exhibit sensitive dependence on initial conditions. According to the theory developed in Refs. 4 and 5 for first-order differential equations, these attractors display distinct Fourier spectral properties. The numerical experiments performed on both first- and second-order ordinary differential equations confirm the theoretical predictions for the Fourier spectra. Furthermore, studies in Refs. 3–6 also showed that strange nonchaotic attractors appear to be typical for quasiperiodically forced systems. By "typical" we mean that they occur on a positive measure set in the parameter space. That is, if we pick a point in the parameter space at random, the system has nonzero probability to yield such an attractor.

There are a variety of ways of characterizing attractors in dynamical systems. Here we review some of them that we will be using in our study.

(i) Equations (2) and (3) have two Lyapunov exponents. One of them, corresponding to Eq. (3) is always zero. The other corresponding to Eq. (2) is

$$\Lambda=\lim_{n\to\infty}\frac{1}{n}\sum_{k=1}^{n}\ln|1+V\cos\phi_k|\ . \tag{5}$$

(ii) The winding number W for an orbit $\{\phi_n\}$ of Eq. (2) is defined as

$$W=\lim_{n\to\infty}\frac{\phi_n-\phi_0}{2\pi n}\ . \tag{6}$$

For $\{\theta_n\}$, the winding number is always ω. Physically, W and ω are the average frequencies with which the orbit circles around in the ϕ and θ directions, respectively.

(iii) Fourier spectra are calculated using a fast Fourier transform (FFT) algorithm[7] applied to the discrete sequence $\{s_n\}_{n=0}^{n=M-1}$, $s_n=h_nP(\phi_n)$, where $P(\phi)=\cos\phi$ and $h_n=[1-\cos(2\pi n/M)]/2$. The multiplication by h_n is a smoothing technique (the so-called method of leakage reduction[7]) which eliminates spurious high-frequency features that would otherwise be introduced by the effective sudden turn-on and turn-off of the Fourier transform operation at the beginning and end of the data string.

To explain the main results of this paper, we refer to the $K-V$ plane diagram shown in Fig. 1 [cf. Eqs. (2) and (3) for the meanings of K and V]. The hatched areas in the diagram indicate the set of parameter values for which the system exhibits negative Lyapunov exponents. According to the qualitatively different dynamical behavior exhibited by Eqs. (2) and (3), Fig. 1 can be divided into three regions. These three regions are separated from each other by two critical curves. The meaning of these curves is discussed below. Region 1 begins at $V=0$ and extends up to the lower critical curve. We see that at $V=0$ the tongues of hatched areas emerge and start to widen as V is increased. These tongues apparently touch each other on a set of points which lie on the lower critical curve. Note that this lower critical curve is below the horizontal line $V=1$ past which the system, Eqs. (2) and (3), becomes noninvertible. Embedded between the hatched tongues are areas where Λ is zero (blank). Corresponding to the hatched and blank areas in Region 1, the attractors exhibited by the system are either two-frequency quasiperiodic ($\Lambda<0$) or three frequency quasiperiodic ($\Lambda=0$). The structure of the K-V plane in this region is similar to that of the circle map Eq. (1) (cf. Sec. II). Between the two critical curves is a region where Λ is always negative. We refer to this region as region 2. Region 2 extends beyond $V=1$ and ends on the upper critical curve. In this region the system exhibits only two-frequency quasiperiodic and strange nonchaotic attractors. Finally, the region above the upper critical curve is referred as region 3. In this region we find only two-frequency quasiperiodic and chaotic attractors (corresponding to blank areas with $\Lambda>0$). In Table I we summarize the results concerning the behavior of Eqs. (2) and (3) on the K-V plane. Notice that the above partition of the K-V plane diagram according to the different dynamical behavior exhibited by the system indicates the importance of the existence of the two critical curves in characterizing the evolution of attractors from three-frequency quasiperiodic to strange nonchaotic to chaotic.

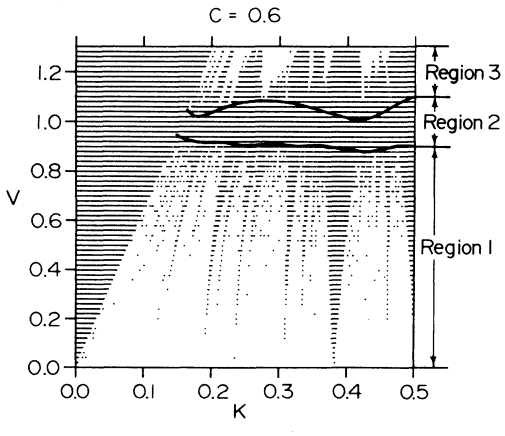

FIG. 1. Diagram of the K-V plane showing the three regions separated by the two critical curves. In region 1, Λ is either negative (hatched) or zero (blank); in region 2, Λ is always negative; in region 3, Λ is either negative (hatched) or positive (blank).

TABLE I. Characterization of the K-V plane. (Two-frequency quasiperiodic attractors exist in all three regions.)

Region	Dynamical behavior	Lyapunov exponent
1	three-frequency quasiperiodic	$\Lambda=0$
2	strange nonchaotic	$\Lambda<0$
3	chaotic	$\Lambda>0$

The organization of this paper is as follows. In Sec. II we give a brief review of the circle map Eq. (1), for comparison with our work on Eqs. (2) and (3) emphasizing the features introduced by quasiperiodic forcing. In Sec. III we present numerical evidence supporting our main conclusion as exemplified by our above discussion of Fig. 1 and Table I. In Sec. IV we present analytical results for the case of strong coupling. In Sec. V we discuss and summarize our conclusions.

II. REVIEW OF THE CIRCLE MAP

If we let $V=0$ in Eq. (1), then the situation is simple. The system exhibits either periodic or quasiperiodic motions, depending on whether K is rational or irrational. Finite V introduces nonlinearity in the system and causes the given periodic orbits to persist for a range of K values. The result is the Arnold tongue structure of the K-V plane shown in Fig. 2. Inside each Arnold tongue, there is an attracting periodic orbit and its winding number satisfies the mode-locking condition: $W=m/n$ with m and n being integers. Between the tongues the winding number W of Eq. (1) is irrational and the system exhibits zero Lyapunov exponent and two-frequency quasiperiodic motions (there are only two frequencies in this sytem). The Arnold tongues touch each other on the critical curve $V=1$. Above this critical curve the tongues overlap and the system can display chaotic attractors.

The decoupled system, $C=0$ in Eqs. (2) and (3), corresponds to the circle map with the phase space dimensionality increased from one to two by the addition of the θ dynamics. This adds an additional frequency to the

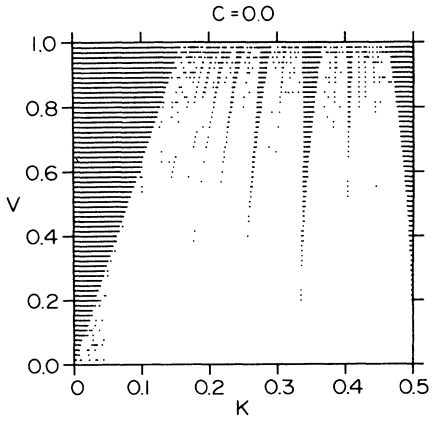

FIG. 2. Diagram of the K-V plane for the circle map Eq. (1) giving regions where $\Lambda<0$ (hatched) and regions where $\Lambda=0$ (blank).

system. Thus, for the expanded system, $C=0$ in Eqs. (2) and (3), the tongues of Fig. 2 correspond to two-frequency quasiperiodic (rather than periodic) motions, and the regions between the tongues correspond to three-frequency quasiperiodic (rather than two-frequency quasiperiodic) motions. Hence, we may regard the region in Fig. 2, $V<1$, as analogous to region 1 of Fig. 1, while the region with $V>1$ (not shown in Fig. 2) is analogous to region 3.

In the case of Eqs. (2) and (3) with $C>0$, the transition from pure quasiperiodicity ($\Lambda=0$) (region 1) to chaos (region 3) is mediated by the existence of a region where strange nonchaotic attractors occur (region 2). Thus we may think of this intermediate transition region (region 2) as the main effect introduced by nonzero quasiperiodic forcing. We shall see that the distance between the two critical curves in Fig. 1 is a function of the quasiperiodic coupling strength C, and that as $C\rightarrow 0$ the two critical curves approach each other and collapse onto $V=1$ when $C=0$.

III. NUMERICAL RESULTS FOR THE QUASIPERIODICALLY FORCED CIRCLE MAP

As mentioned in Sec. I, there exist two critical curves in the K-V plane which delineate the transition between qualitatively different dynamical behavior. In this section we present our numerical work supporting this and other associated results, and we use examples to illustrate the distinct characteristic properties of the different kinds of attractors that can arise in typical quasiperiodically forced dynamical systems. We also present detailed arguments on the existence of strange nonchaotic attractors in terms of Lyapunov exponents and winding numbers.

A. Lyapunov exponents and winding numbers

The K-V plane shown in Fig. 1 was obtained by taking a grid with 320 values of K and 65 values of V; the orbit length varies from 10^4 to 6×10^5, depending on the convergence of the Lyapunov exponents. The criteria for negative, positive, or zero Lyapunov exponents used in Fig. 1 are $\Lambda<-0.000\,05$, $\Lambda>0.000\,05$, or $-0.000\,05<\Lambda<0.000\,05$. With the grid used we find no parameter values in region 3 for which the system exhibits "zero" Lyapunov exponents. Thus the set of parameter values on which $\Lambda=0$ apparently has zero measure in region 3. We note that the two critical curves, upper and lower, are drawn to indicate the existence of the partition of the K-V plane into three regions, and these critical curves are not uniquely determined based on our numerical data.

In Fig. 3 we plot W and Λ as functions of K for fixed V and C in region 2 (the region of two-frequency quasiperiodic and strange nonchaotic attractors). The orbit length used is 10^5. The W versus K curve, Fig. 3(a), is apparently a "devil's staircase": a continuous nondecreasing curve with a dense set of open intervals on which W is constant and given by

$$W=\frac{m}{n}+\frac{l}{n}\ , \tag{7}$$

where m, l, and n are integers. Between these intervals there is a Cantor set on which W increases with K. The Λ versus K curve is given in Fig. 3(b), where all the Lyapunov exponents are negative. Since W is a continuous nondecreasing function of K, it certainly crosses the

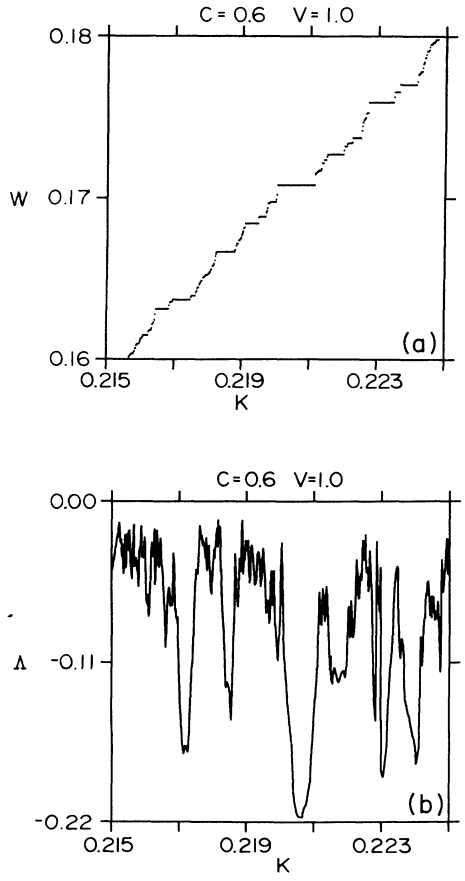

FIG. 3. Curves of (a) winding number (W) vs K and (b) Lyapunov exponent (Λ) vs K for $C=0.6$ and $V=1$.

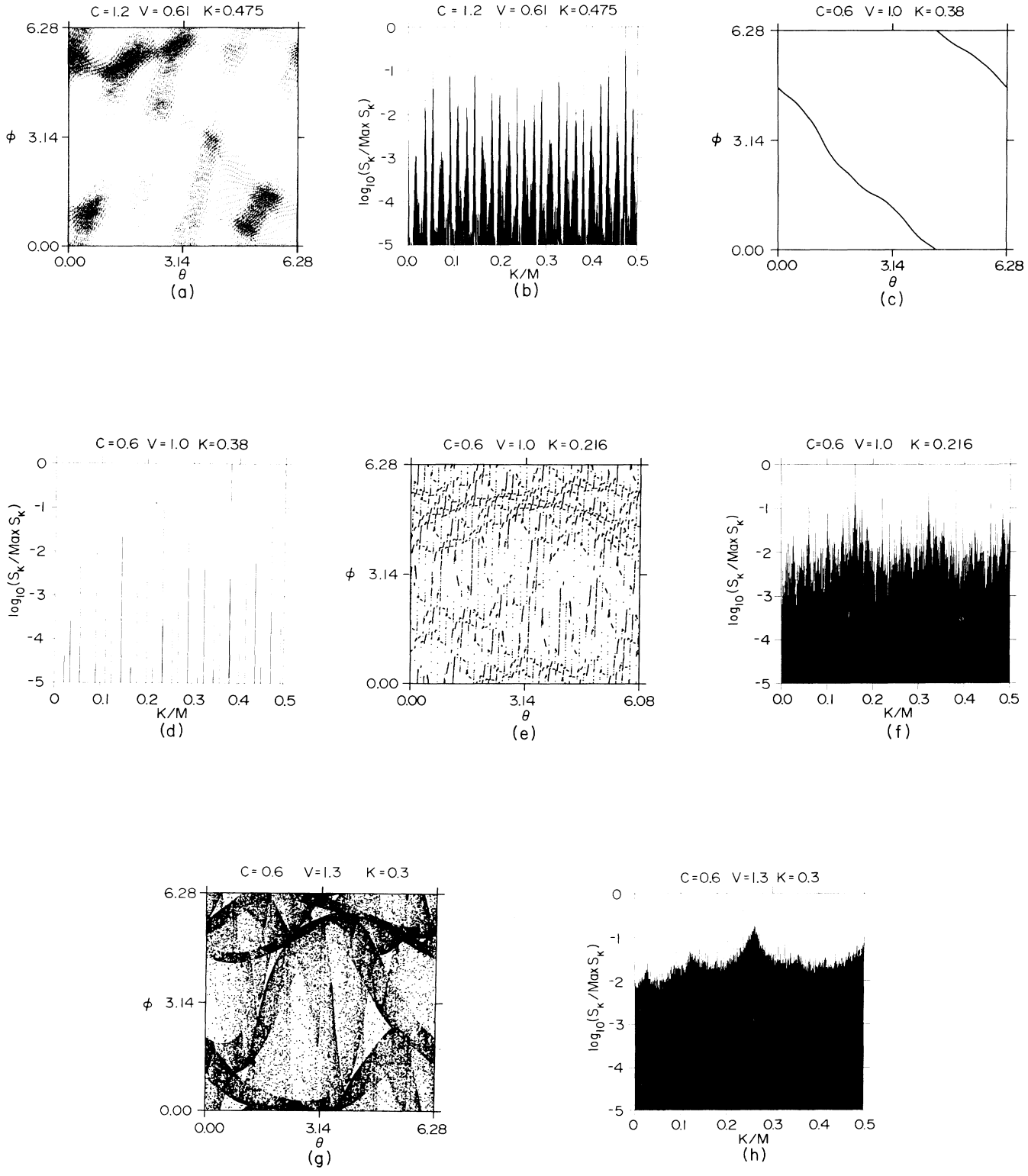

FIG. 4. Phase space plots and frequency spectra corresponding to orbits on a three-frequency quasiperiodic attractor for $C=1.2$, $V=0.61$, and $K=0.475$ [(a) and (b)], a two-frequency quasiperiodic attractor for $C=0.6$, $V=1.0$, and $K=0.38$ [(c) and (d)], a strange nonchaotic attractor for $C=0.6$, $V=1.0$, and $K=0.216$ [(e) and (f)], and a chaotic attractor for $C=0.6$, $V=1.3$, and $K=0.3$ [(g) and (h)].

points where Eq. (7) does not hold. This combination of negative Lyapunov exponent and the irrational relationship between W, ω, and 1 is the criterion for the existence of strange nonchaotic attractors.

If we decouple Eq. (2) and Eq. (3) by letting $C=0$, the resulting system is the circle map [Eq. (2)] with an additional dimension expanded by θ and its corresponding frequency ω. In this decoupled case, since the motion along the ϕ direction is not affected by the motion along the θ direction, the mode-locking condition Eq. (7) reduces to its subset where $W=m/n$ and $l=0$. As we have already seen in Sec. II, this subset corresponds to the mode-locking condition of the circle map. Therefore, on the K-V plane, nonzero quasiperiodic coupling in Eq. (2), allowing nonzero l in Eq. (7), introduces more mode-locking tongues than in the case of the circle map. (This may be the reason why the lower critical curve in Fig. 1 occurs below $V=1$ which is the only critical curve for the circle map.)

B. Phase space plots and Fourier spectra

For regions 1 and 2 the three distinct combinations of winding numbers [either satisfying Eq. (7) or not] and Lyapunov exponents (either negative or zero) give rise to phase space plots and Fourier spectra with qualitatively different characteristics, as summarized in Table II.

In case A the three frequencies W, ω, and 1 are irrationally related and the Lyapunov exponents are zero; therefore the system exhibits three-frequency quasiperiodic behavior. A typical orbit generates a smooth density of points densely filling the (θ,ϕ) plane as illustrated in Fig. 4(a). In Fig. 4(b) we plot the frequency spectrum corresponding to the orbit shown in Fig. 4(a).

In case B the frequencies W, ω, and 1 are rationally related and the corresponding Lyapunov exponents are negative, therefore the system exhibits two-frequency quasiperiodic attractors. The attractor in the (θ,ϕ) plane lies on a smooth multivalued curve. If we take in Eq. (7) l,n and m,n to be relatively prime integers, then n gives the multiplicity of the curve in the ϕ direction and l gives the multiplicity of the curve in the θ direction. An example of a two-frequency quasiperiodic attractor is given in Fig. 4(c), and in this case $(n,l,m)=(1,-1,1)$. Figure 4(d) shows the frequency spectrum for the orbit in Fig. 4(c).

In case C the attractor is geometrically strange: It satisfies the functional relation $\phi=F(\theta)$. F can be a multivalued function. But F is discontinuous everywhere (hence strange). This can be verified in the following way. (i) To verify the existence of the relationship $\phi=F(\theta)$ we initialize a large number of points at a single initial θ value but with different initial ϕ values and find that after a large number of iterates N, all the orbits are attracted to a set of values $\phi_N^{(i)}$, where $i=1,2,3,\ldots,P$ and P is the multiplicity of the function F. (ii) That $\phi=F(\theta)$ cannot be a continuous function follows from the fact that the winding number W is irrationally related to 1 and ω. (iii) Finally, that $\phi=F(\theta)$ is discontinuous everywhere results from the fact that the map Eq. (3) is ergodic (so if F is discontinuous anywhere it is discontinous everywhere). An example of a strange nonchaotic attractor and its corresponding frequency spectrum is given in Figs. 4(e) and 4(f).

Note that the spectrum of the two-frequency quasiperiodic attractor, Fig. 4(d), is concentrated on a small discrete set of frequencies, while the spectra of both the three-frequency quasiperiodic [Fig. 4(b)] and strange nonchaotic attractors [Fig. 4(f)] apparently have comparatively much richer harmonic content.

It is interesting to note that the information dimension of strange nonchaotic attractors, as predicted by the Kaplan-Yorke formula,[8,9] is unity. However, as will be shown in a future publication,[10] there is evidence indicating that the capacity (box-counting) dimension is two for these attractors.

The three types of attractors discussed above can arise in quasiperiodically forced systems which do or do not allow chaotic attractors to exist. In the case of Eqs. (2) and (3), which we believe is typical of the quasiperiodically forced systems which allow chaotic attractors to exist, chaos (i.e., $\Lambda>0$) is the state the system might transit to from strange nonchaotic attractors as a parameter is varied (e.g., V is increased so as to cross the upper critical curve). Figures 4(g) and 4(h) are examples of a chaotic attractor and its corresponding Fourier spectrum.

The phase space plots in this section, Figs. 4(a), 4(c), 4(e), and 4(g), are generated by plotting long orbits ($N=4\times10^4$ to 2×10^5) in the (θ,ϕ) plane after discarding the initial 4000 iterates (to eliminate the effect of transients). The Fourier spectra, Figs. 4(b), 4(d), 4(f) and 4(h), are obtained by using an fft algorithm (cf. Sec. I) with $M=2^{15}$.

IV. ANALYTICAL RESULTS FOR LARGE C

To gain insight for the case $C\gg V$, neglect the "$V\sin\phi_n$" term in Eq. (2). The result is

$$\phi_{n+1}^0=[\phi_n^0+2\pi K+C\cos\theta_n]\ , \tag{8}$$

$$\theta_{n+1}=[\theta_n+2\pi\omega]\ . \tag{9}$$

Since the average of $\{\cos\theta_n\}$ is zero the winding number W^0 of Eq. (8) is

$$W^0=K\ . \tag{10}$$

TABLE II. Characteristics of attractors.

Case	Winding number	Lyapunov exponent	Type of attractors	Figures
A	$W\neq\frac{m}{n}+\frac{l}{n}\omega$	$\Lambda=0$	three-frequency quasiperiodic	4(a) and 4(b)
B	$W=\frac{m}{n}+\frac{l}{n}\omega$	$\Lambda<0$	two-frequency quasiperiodic	4(c) and 4(d)
C	$W\neq\frac{m}{n}+\frac{l}{n}\omega$	$\Lambda<0$	strange nonchaotic	4(e) and 4(f)

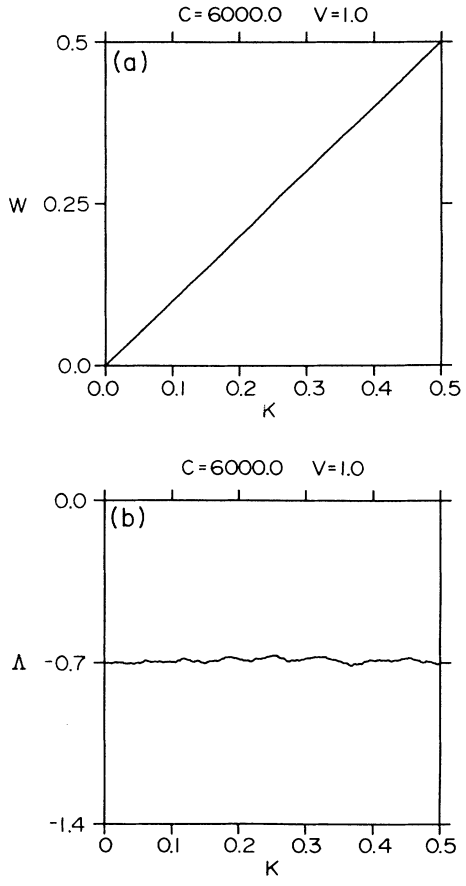

FIG. 5. Curves of (a) winding number (W) vs K and (b) Lyapunov exponent (Λ) vs K for $C=6000$ and $V=1$.

Figure 5(a) shows the W versus K curve for the system of Eqs. (2) and (3) with $C=6000$. All the points lie approximately on the diagonal line $W=K$, as predicted by Eq. (10).

In Eq. (5) if we use the orbit $\{\phi_n^0\}$ obtained from Eq. (8) instead of the actual orbit $\{\phi_n\}$ obtained from Eq. (2) we get

$$\Lambda^0=\lim_{n\to\infty}\frac{1}{n}\sum_{k=1}^{n}\ln|1+V\cos\phi_k^0| =\frac{1}{2\pi}\int_0^{2\pi}\ln|1+V\cos\phi|d\phi\ , \tag{11}$$

where the last step is arrived due to the fact that $\{\phi_n^0\}$ is uniformly distributed on $[0,2\pi]$.

Performing the integral in Eq. (11) yields

$$\Lambda^0=\begin{cases}-\ln\{2/[1+(1-V^2)^{1/2}]\}, & V\le 1\\ \ln(V/2), & V\ge 1\ .\end{cases} \tag{12}$$

Figure 5(b) shows the numerically computed Λ as a function of K for $C=6000$ and $V=1$. All points are concentrated near the value $\Lambda^0=-0.693$ predicted by Eq. (12).

Finally for $V>2$, Eq. (12) predicts $\Lambda^0>0$. Indeed we find for $V>2$ and large C that the system Eqs. (2) and (3) exhibits chaotic attractors. Therefore $V=2$ is the upper critical curve marking the transition from strange nonchaotic attractors to chaotic attractors for large C.

These results together with the discussion of Sec. II suggest the following picture of what happens as the coupling C varies: For $C\to 0$ the two critical curves collapse onto the line $V=1$. As C increases they move apart and region 2 enlarges. For $C\to\infty$ the upper critical curve approaches $V=2$, while the lower critical curve approaches $V=0$, squeezing region 1 onto the V axis.

V. CONCLUSIONS

In this paper we discuss the existence of strange nonchaotic attractors for the quasiperiodically forced circle map Eqs. (2) and (3). Various numerical experiments are performed to illustrate the different types of attractors that can arise in typical quasiperiodically forced systems. The central result is that in the two-dimensional parameter plane of K and V, the set for which the system Eqs. (2) and (3) exhibits strange nonchaotic attractors has Cantor-like structure and is embedded between two critical curves. One of these curves marks the transition from three-frequency quasiperiodic attractors to strange nonchaotic attractors; the other marks the transition from strange nonchaotic attractors to chaotic attractors. This forms a possible route to chaos in two-frequency quasiperiodically forced dynamical systems, namely, (three-frequency quasiperiodicity)→(strange nonchaotic behavior)→(chaos).

ACKNOWLEDGMENTS

This work was supported by the U.S. Department of Energy (Basic Energy Science) and the Office of Naval Research (Physics Division).

[1]See, for example, P. Bak, T. Bohr, and M. H. Jensen, Phys. Scr. **T9**, 50 (1985).

[2]J. P. Sethna and E. D. Siggia, Physica D **11**, 193 (1984); S. Wiggins, Phys. Lett. **A124**, 138 (1987); K. R. Meyer and G. Sell (unpublished).

[3]C. Grebogi, E. Ott, S. Pelikan, and J. A. Yorke, Physica D **13**, 261 (1984).

[4]A. Bondeson, E. Ott, and T. M. Antonsen, Phys. Rev. Lett. **55**, 2103 (1985).

[5]F. J. Romerais, A. Bondeson, E. Ott, T. M. Antonsen, and C. Grebogi, Physica D **26**, 277 (1987).

[6]F. J. Romeiras and E. Ott, Phys. Rev. A **35**, 4404 (1987).

[7]E. O. Brigham, *The Fast Fourier Transform* (Prentice-Hall, Englewood Cliffs, NJ, 1974).

[8]J. Kaplan and J. A. Yorke, *Functional Differential Equations and the Approximation of Fixed Points* (Springer, Berlin, 1978), p. 288.

[9]J. D. Farmer, E. Ott, and J. A. Yorke, Physica D **7**, 153 (1983).

[10]M. Ding, C. Grebogi, and E. Ott (unpublished).